

Article

Brightly Colored to Stay in the Dark. Revealing of the Polychromy of the Lot Sarcophagus in the Catacomb of San Sebastiano in Rome

Susanna Bracci ^{1,*}, Donata Magrini ^{1,†}, Rachele Manganelli del Fà ^{1,†},
Oana Adriana Cuzman ^{1,†} and Barbara Mazzei ^{2,†}

¹ Institute for Heritage Science, National Council of Research–ISPC-CNR, Via Madonna del Piano 10, 50019 Sesto Fiorentino, Italy; donata.magrini@cnr.it (D.M.); rachele.manganellidelfa@cnr.it (R.M.d.F.); oanaadriana.cuzman@cnr.it (O.A.C.)

² Pontificia Commissione Archeologia Sacra, Via Napoleone III 1, 00185 Rome, Italy; bmazzei@arcsacra.va

* Correspondence: susanna.bracci@cnr.it

† These authors contributed equally to this work.

Received: 18 June 2020; Accepted: 21 July 2020; Published: 27 July 2020



Abstract: The Lot Sarcophagus is one of the most relevant funerary sculptures of late antiquity (mid-4th century AC). Some of the remarkable aspects are the following (i) it is still preserved in situ; (ii) most of the carved scenes are rarities or unicum; (iii) not all the sculpture work has been completed, which allows us to analyse the executive process; (iv) many traces of polychromy have remained. This paper is focused on the characterization of the residual polychromy by using in-situ non-invasive techniques. Furthermore, few micro samples were taken, to be analysed in laboratory to study the composition of some deposits and to define if a preparatory layer was present under the coloured layer. The data showed that the very rich polychromy of the Lot Sarcophagus was made of Egyptian blue, yellow ochre, and three different types of red: two inorganics (red ochre and cinnabar), and one organic-based (madder lake). Furthermore, some decorations, completely vanished and no longer visible to the naked eye, have been rediscovered, also providing details on the construction phases. During the project, the 3D model of the sarcophagus was acquired, which afterwards was used to map the results of the diagnostic campaign.

Keywords: Lot Sarcophagus; polychromy; non-invasive analyses; archaeometry; conservation

1. Introduction

Although many ancient civilizations are known to have made use of polychromy on stone sculptures and architectural elements [1], most of these colours were lost.

After a period of mistaken interpretation of sculpted objects as pure white, a long discussion among scholars, about if ancient objects were painted or not, began in 1800 and continued throughout the past century. In recent years, the interest in the study of original polychromy on ancient stone artefacts has grown. This work is included in a wider research project aimed to enlighten the use of colours on the sculptures in Roman time.

Gathering as much information as possible about the original polychromy of an archaeological find is extremely important as it offers a new key that gives scholars and the public the sculpture's original appearance.

A correct understanding of the original polychromy is complicated by the fact that the few traces of residual colour are often small due to the vicissitudes the sculptures underwent, such as burial for hundreds or thousands of years, excavation and exposure to the environment, bad storage, and severe cleaning treatments.

During previous years, both non-invasive and micro-invasive techniques and their combinations were applied to characterize remnant materials and pigments on polychrome objects [2,3]. In particular, imaging techniques have become part of the set of analytical methodologies available for the investigation of objects in archaeological contexts [4–9]. Among these techniques, ultraviolet-induced luminescence (UVL) and visible-induced luminescence (VIL), both photographic methods, are being progressively adopted by a wider range of users including scientists, conservators, archaeologists, and curators. The extensive use of these techniques is the result of the rapid development of digital cameras, with easier image acquisition and control of parameters. UVL is a well-documented photographic technique widely used to characterize varnishes and integrations on paintings [10–16]. It is also used by scholars to rapidly detect materials on stone surfaces and has increasingly become part of analytical protocols to study colour traces on ancient artefacts.

Egyptian blue, a synthetic pigment, whose recipe dates to the first dynasties of ancient Egypt, beginning about 3100 BC, is one of the oldest known synthetic pigments [17,18]. Egyptian blue absorbs visible radiation and re-emits a broad and intense band in the infrared (IR) range, at about 910 nm. VIL, quite a recent technique set up by Verri [19–22], takes advantage of this peculiar feature that allows us to reveal Egyptian blue and to distinguish it from other blue pigments. Observing the image on a grey scale, Egyptian blue appears bright white while other pigments and materials appear from light to dark grey. The pigment emission is so strong that its luminescence can be easily identified and localized with a modified camera, even if the pigment is present in traces no longer visible to the naked eye.

The use of imaging techniques allows the gaining of a large amount of information, but it is advisable that the examination also includes the use of other non-invasive analytical techniques in order to implement the data and integrate the results obtained [23,24]. Among non-invasive portable techniques, nowadays available, spectroscopic ones such as infrared spectroscopy in total reflection mode (TR FT-IR) [25], fibre optic reflectance spectroscopy in the UV–VIS–NIR range (FORS) [26–29], or X-ray fluorescence (XRF) [30,31], are widely applied for the study of the remains of original polychromy [32]. Furthermore, if micro sampling is required, thanks to the preliminary application of non-invasive techniques, it is possible to perform it in a more rational and limited way.

2. The Lot Sarcophagus

The Lot Sarcophagus, still preserved in situ, is made by a monolithic lid with a frieze on the front and by a monolithic chest with a double register frieze on the front, interrupted in the centre by a shell containing two portrait busts (Figure 1).

The sculpted artwork dates to the mid-4th century AC, since the stylistic manner seems to demonstrate it was produced by a thriving Roman marble workshop [33].

The Lot Sarcophagus was found in June 1950 during the excavation, conducted by Father Ferrua, of a sumptuous mausoleum adjacent to the Basilica of Saint Sebastian. The sarcophagus was positioned about 2.60 m under the soil and, all around it, was protected by a strong masonry. Over the lid there was also another type of less resistant masonry, which Ferrua thought had been done when the sarcophagus was reopened to insert a second deceased. Between the masonry and the sculpted surface there was a layer of lime mortar that was removed by the discoverers with hard chisel work, leaving some traces over the surface. After the excavation, many colour traces disappeared [34].

During recent conservation work, the entire marble surface was cleaned in a respectful and non-invasive way towards both the colors and the marble surface¹. This allowed the recovery of many colour traces under the residue lime mortar [35].

¹ The restoration was conducted by Serena Di Gaetano, a private restorer whom we thank for the delicate and punctual work done.

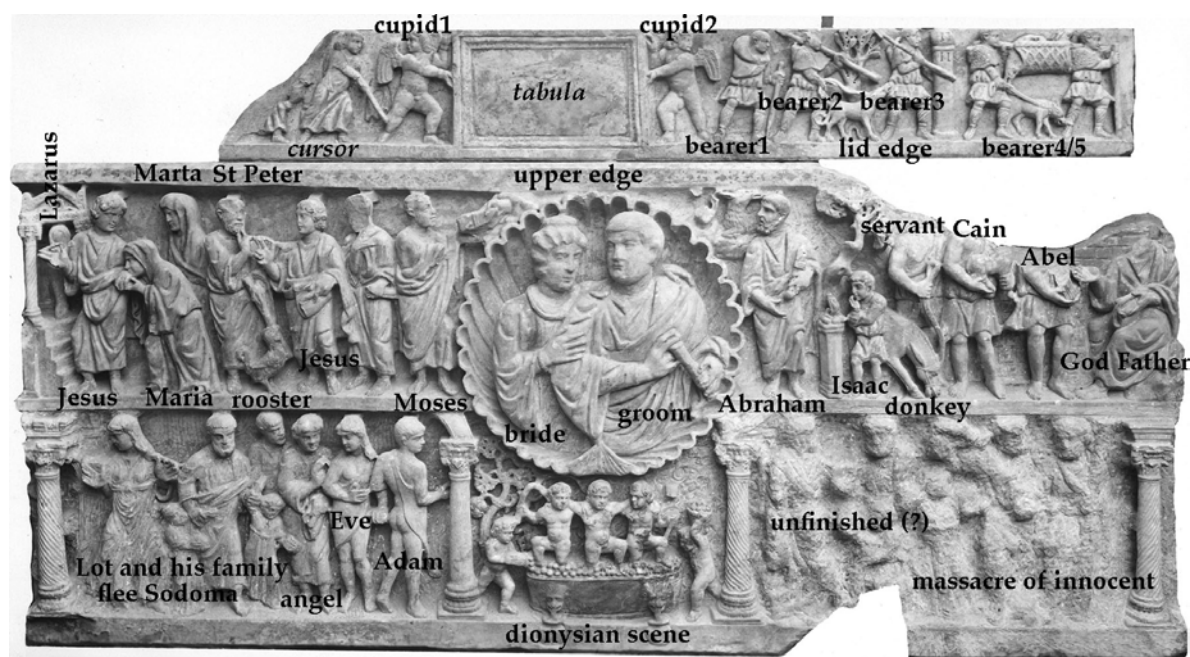


Figure 1. Image of the front of the Lot Sarcophagus with the indications of the names of the characters represented.

The frieze on the lid shows a group of bearers returning to the city after the hunt. In the centre of the frieze two cupids held a *tabula*, unfortunately without any inscription.

On the chest, in the upper register and on the left side, Christ raising Lazarus, in the presence of Mary (Lazarus' sister) and Martha, Peter (with the rooster at his feet) denying Jesus, and Moses receiving the Law are represented. On the right side: Abraham who is about to sacrifice his son Isaac, a servant with a donkey and Cain and Abel offering the gift of their work to God the Father. In the centre of upper register, there is a shell where the couple buried in the sarcophagus, whose names are not known, is probably portrayed. The lower register is very interesting because it shows unusual scenes and the relief is not completely carved. On the left of the Lot, his family flee Sodom and the scene of God's angel ordering Adam and Eve to leave the Garden of Eden, are represented. Below the central shell, the dionysiac scene of the pressing of the grapes is displayed. In the last sector, which is barely outlined, we can recognise only the massacre of the innocents on the far right, while the previous scene remains uncertain.

3. Materials and Methods

The analytical protocol was based on two diagnostic phases. The first one was based on the in-situ application of the multi band photographic techniques (UVL and VIL) and two non-invasive spectroscopic techniques: X-ray fluorescence (XRF) and fibre optic spectroscopy (FORS). At the same time, the images for creating the 3D model were acquired. The digital model was later used to map the diagnostic data, and this application is described in an article currently being drafted. In the second phase, after the collection and evaluation of the data, for the still unsolved questions, micro samples were taken and, afterwards, analysed in a laboratory.

3.1. In-Situ Instrumentation

For the photographic UVL, a digital camera Canon EOS 7D (18 Mpixel, CMOS sensor) was used. The camera was equipped with a Canon lens EFS 28 mm f/3.5 with a B+W486 UV/IR blocking filter to cut reflected ultraviolet. As sources, two Flash Quantum T5D with B+W UV black 403 filters were used. The same set-up was used for acquiring visible images removing the filter from the flashes.

For VIL acquisitions, the surfaces were irradiated with visible light by using two flashes Quantum T5D mounted with a B+W 486 UV/IR blocking filter, the infrared luminescence was collected with a modified (built-in filter for IR removed) Canon EOS 400D (10.1 Mpixel, CMOS sensor) with Canon lens EFS 28 mm with a B+W 093 infrared filter to cut all stray radiation from the visible spectrum and thus collecting only infrared luminescence. A white Spectralon[®] plate (WS-1S-L Labsphere certified standard) was used as reference.

Digital images were acquired in situ by a portable microscope Scalar DG-2A equipped with optical zoom with magnifications from 25× to 200×. This was used for the documentation of both measured areas and details. Images were acquired at 25× magnification (investigated area of 13 × 8 mm).

Fibre optic reflectance spectroscopy (FORS) measurements were carried out in the spectral range 350–900 nm by using a tungsten lamp (20 W) as the source and the grating Ocean Optics (model HR2000) as the detector connected by optical fibre bundles Y shaped. The measuring head geometry was chosen as small as possible due to fact that the sculpted surface presented very few flat areas. Therefore, the head configuration for the measure was 0/0°. The probe head in contact with the surface was supplied with a homemade black cylinder, which, at the same time, guarantees a soft contact, permits the fixing of the best distance from the surface in order to maximise the signal, and maintains the measuring area shielded from undesired external light. The analysed area was 2 mm in diameter, each acquired spectrum was the average of 30 scans. As reference, a Spectralon[®] plate was used. Spectra were compared with reference ones available in the ISPC-CNR reference database to identify pure pigments or admixtures.

The X-ray fluorescence (XRF) spectra were collected by means of handheld Tracer III SD Bruker spectrometer, equipped with rhodium anode and a solid-state silicon detector energy dispersion system. The used set-up was 40 keV and 12 µA for 120 s. The measuring area was an elliptical spot of 4 × 7 mm. For data processing, ARTAX software was used. As far as possible, efforts were made to acquire the measurements with the two spot techniques (XRF and FORS) on the same area also taking into account that the dimensions of the investigated areas are different for the two techniques.

One of the criteria for choosing these techniques is their flexibility to be used in unconventional conditions, such as those of the environment of the sarcophagus, inside the catacomb, where the conditions were rather harsh (temperature range 12–15 °C, RH 90–95%). The number of in situ analyses is reported in Table 1.

Table 1. Number of in-situ analyses.

Technique	Number of Acquisitions	
Multi band imaging	Vis	63 photos
	UVL	30 photos
	VIL	33 photos
Digital optical microscopy	53 photos	
FORS UV-Vis	40 spectra	
XRF	31 spectra	

The digital model of the sarcophagus was created by using Agisoft PhotoScan (<http://www.agisoft.com/>), a software that performs photogrammetric processing of digital images [36] generating 3D spatial data. For the sarcophagus and the surrounding environment, about 200 photos were acquired using a Nikon D3300 (24,2 Mpixel, CMOS sensor) equipped with a Nikkor lens AF-S 18–55 mm.

3.2. Laboratory Instrumentation

An optical microscope Nikon Eclipse E600 was used for the acquisition of images of the micro samples collected in both visible reflected light and UV (filters λ_{ex} 330–380 nm; λ_{em} > 410 nm).

FT-IR spectra were recorded using an Alpha Bruker Optics Spectrophotometer by using an Attenuated Total Reflectance (ATR) module equipped with a diamond crystal. For each spectrum,

64 scans were acquired in the spectral range 4000–375 cm^{-1} , with 4 cm^{-1} resolution. All the spectra were processed by using the ATR correction tool for ATR diamond crystal with the Opus 7.0.122 software by Bruker Optics.

Scanning Electron Microscope (SEM) measurements were performed with a FEI-ESEM-Quanta 200 instrument in low vacuum (1 Torr). It was equipped with both secondary and back-scattered electron detectors and with EDS detector for micro-analysis. The electrons in the primary beam were accelerated with a potential difference of 25 keV.

Samples for studying the biological growth were taken by using sterile cotton swabs. The samples were then sown in a laboratory by passing the swab directly on nutrient media. Potato Dextrose Agar (PDA, Difco™) was used to detect a possible fungal presence, whereas a liquid BG11M nutrient medium was used to detect a possible phototrophic presence. The latter nutrient medium was prepared according to Rippka [37], which was then adjusted with 5 mL/L of NaNO_3 . The morphological characterization was made by using a Nikon Eclipse E200 microscope, according to Komarek et al. [38,39].

4. Results

As already described, at the time of the discovery (June 1950), the sarcophagus was buried in a niche under the floor of the mausoleum. Between the walls of the sarcophagus and the walls of the niche there was a tenacious and very adherent masonry, as reported by Father Ferrua [34].

Microsamples of both white and brownish materials, deposited either on marble or on painting traces, were analysed by means of FT-IR in ATR mode. They were all constituted by calcite (CaCO_3) together with some silicates. Therefore, these samples (Table 2) were identified as residues of the masonry mentioned at the time of the excavation and not completely removed.

Table 2. Objective of sampling, number of samples, and summary of results.

	Number of Samples	Colour	Analytical Technique(s)	Results
Biological identification	2	blue	cultivation	<i>Phormidium</i> sp. coccoid cyanobacteria
Deposits identification	3	white-brownish	FT-IR ATR	Calcite Silicates
		yellow		Single layer–no preparatory layer Yellow ochre
Stratigraphy (cross sections)	3	red	SEM-EDS FT-IR ATR	Layer 1–red cinnabar, red ochre, lead white, red lake Layer 2–white preparatory layer lead white
		purple		Single layer–no preparatory layer umber, cinnabar, and Egyptian blue

UVL images acquired covered most of the surface of the sarcophagus. In many cases, the same area was investigated not only by positioning the set up in front of the surface but also with different orientations since the traces were also found in the most hidden areas of the sculptures.

In the UVL images, in particular of the first and second register of the surface, several circular spots of different dimensions, characterized by a brilliant red luminescence emission, were evidenced. As an example, both the Vis and UVL images acquired on the tabula, the hand, and the arm of the cupid2 are reported in Figure 2a–d. These red spots in UVL were supposed to be due to a biological growth, appearing to be of a blue–green color in the VIS images (Figure 2a,c, and Figure 3).



Figure 2. (a) Vis and (b) UVL images of the tabula and (c) Vis and (d) UVL images of cupid2. First register of the sarcophagus. The arrowheads indicate the blue–green biological growth.

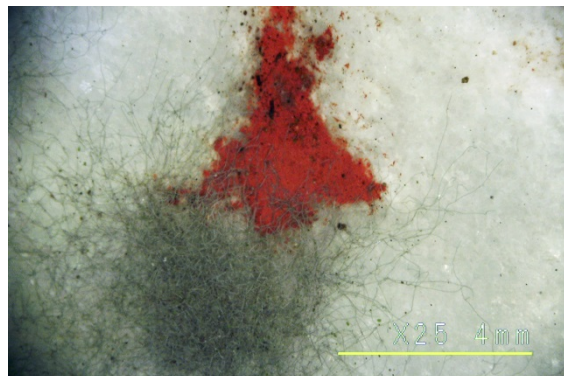


Figure 3. Detail of the biological growth (grey filaments) partly overlapping the red color of the Roman numeral of the milestone on the right of the first register (Vis image acquired with digital OM, 25 \times , bar = 4 mm).

The identification of the spots of supposed biological origin, was made through laboratory cultivation techniques (Table 2). No fungal growth was observed on the PDA medium after two weeks of incubation time. Filamentous cyanobacteria such as *Phormidium* sp. and round-shaped coccoid colonial cyanobacteria were detected in the BG11M nutrient medium. This kind of bacteria is characterized by a very efficient photosynthetic apparatus able to grow in dim light conditions at very low light levels (10–15 lux) [40,41]. The photosynthesis efficacy and the colonization velocity are influenced by the light wavelength. Therefore, this feature could be used to control the possible regrowth after the restoration process by using blue sources for lighting [42,43]. These colonizers of harsh environments contain photosynthetic pigments, mainly chlorophylls and phycobiliproteins, the latter giving the blue–green color in visible light. The characteristic red fluorescence under the UV light, is instead due to the presence of chlorophylls.

Therefore, when looking at UVL images, attention must be paid to the presence of this biological growth to distinguish it by those materials that have a similar color in UVL images but were, on the contrary, intentionally applied.

Indeed, in UVL images, a red fluorescence was also present in several of the areas colored in hues from pink to red in visible light, but also in some areas in which the colour was no longer visible to the naked eye. In Figure 4, images of the cupid1 and the cloth of Abel are reported. The cupid1 shows red fluorescence on the wing, the lips, and the eye, while in the cloth of Abel the fluorescence is evident both on the folds and the belt.



Figure 4. (a) Vis and (b) UVL images of the cupid1 (first register). (c) Vis and (d) UVL images of the cloth and belt of Abel (second register).

Through the spot analyses (FORS and XRF) it was possible to identify the presence of three different kind of red pigments. The FORS spectra acquired in those areas characterized by a pink/red UV luminescence indicate the use of a red lake, likely madder lake [44,45]. As an example, in Figure 5c the FORS spectrum acquired on the line decorating the milestone (red 1, Figure 5a, red line) is reported. Red lake has been widely used for the decoration of figures carved on the lid, for example for the dress of the cursor, that was completely painted in red, and for the edges and folds of the clothes of the bearers on the right. In addition, red lake was used to underline most of the details of the faces (lips and eyebrows), the wings of the cupids, and the linear decorations of the edge of the lid. Less traces of red lake were found in the second register, a linear decoration on the upper edge of the sarcophagus, the belt and cloth of Abel, the underlining of the edges of the stones of the wall behind the legs of Cain, and Abel and God the Father. No traces of red lake were found in the third register.

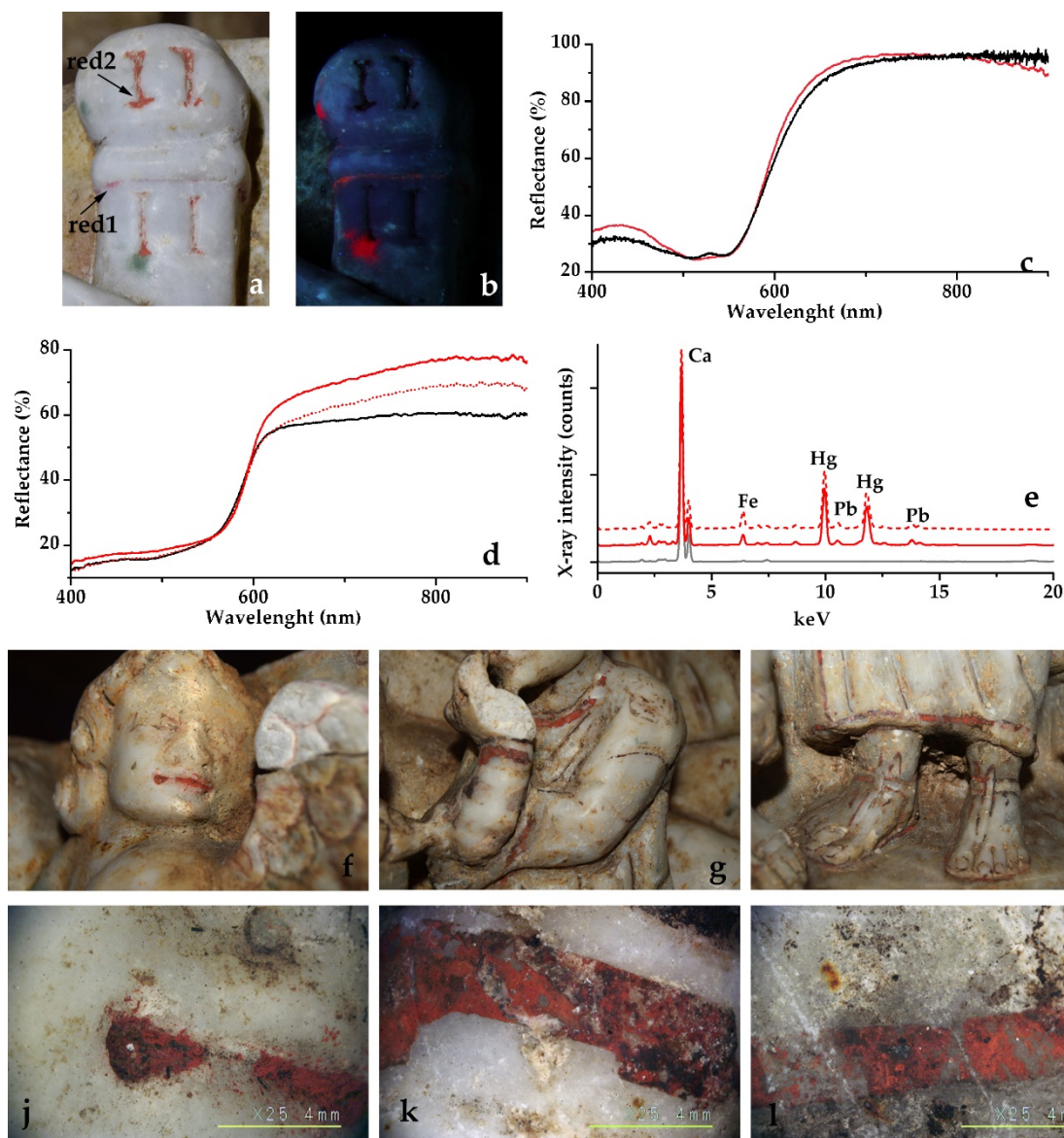


Figure 5. (a) Milestone with the indication of red1 and red2 and (b) UVL image of the same area. (c) FORS spectrum of red1 (red line) compared to a reference spectrum of madder lake (black line). (d) FORS spectra of two areas of red2 (solid and dotted red lines) compared to a reference spectrum of cinnabar (black line). (e) XRF spectra of two areas of red2 (solid and dotted red lines) compared to a spectrum acquired on white marble (grey line). (f–i) Areas painted with cinnabar and (j–l) details of the same areas acquired with a digital microscope (25X, bar = 4 mm).

Other red traces present (i.e., Roman numeral on the milestone, red 2, Figure 5a) appeared black in the UVL images (Figure 5b). The acquired data are reported in Figure 5d,e. The FORS spectra (Figure 5d), acquired in two areas on the Roman numeral show the characteristic “S shape” of cinnabar (HgS) [28,29], with the inflection point @ 595 nm (inflection point of reference cinnabar @ 598 nm). Moreover, in the XRF spectrum of the same areas (Figure 5e), signals of mercury (Hg) are clearly visible. Apart from the Roman numeral on the milestone and the lips of the cupid2 (Figure 5f,j), both belonging to the lid, cinnabar was found mainly in the second register, for the edges of the clothes of the characters (Figure 5g,i,k,l), for a line decorating the steps of the tomb of Lazarus on the left, and for the outline and decorations of the shoes of the characters on the left of the central shell (Figure 5i). No traces of cinnabar were found in the third register.

Observing the XRF spectra in Figure 5e, together with signals of calcium (Ca) and mercury (Hg), iron (Fe, low amount) and lead (Pb, traces) were detected. The iron (Fe) was present in almost all the areas where cinnabar was also identified but its amount was variable. The presence of this element could have been due to the prolonged contact of the surfaces with the earth and the masonry previously described. Yet, in the XRF spectra acquired in areas of the marble without traces of paint, the iron counts were absent (Figure 5e, grey spectrum) and this could suggest an intentional use, even if in different amounts, of red ochre blended with cinnabar.

Red ochre (red3) was identified in the traces of the decorations of the frames, the central part of the *tabula* (Figure 2a), and in Isaac's hair, as the only red pigment used. In Figure 6a,b the FORS and XRF spectra acquired in these two areas are reported. FORS spectra are characterized by the typical shape of red ochres with absorption bands of about 680 and 870 nm due to hematite (Fe_2O_3) [28,46].

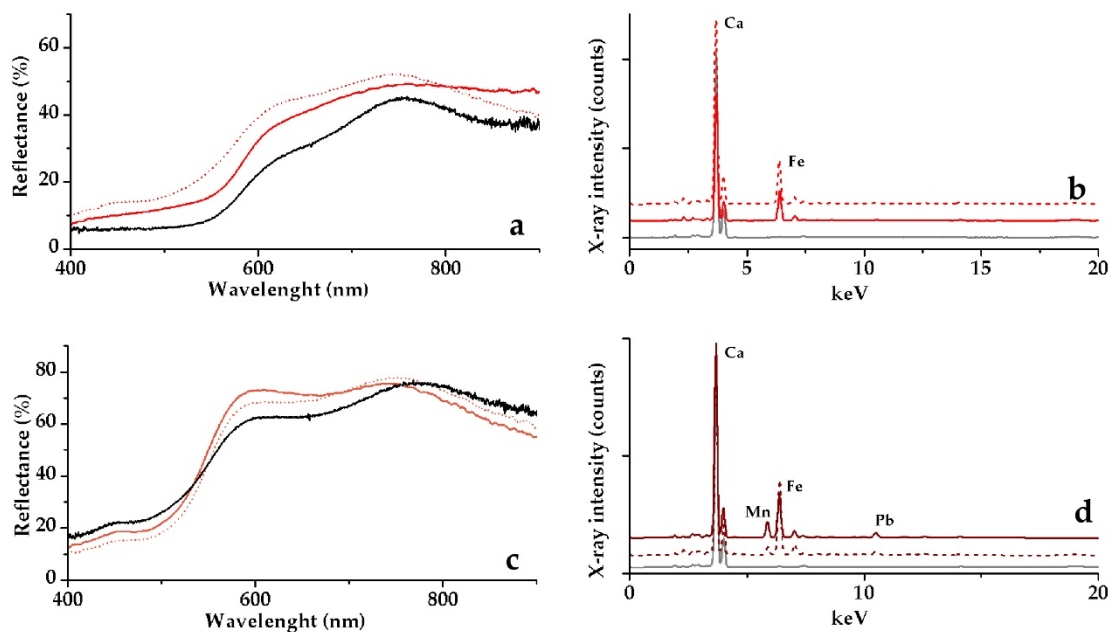


Figure 6. (a) FORS spectra of two areas of red3 (solid and dotted red lines) compared to a reference spectrum of red ochre (black line). (b) XRF spectrum of red3 (solid red line) compared to a spectrum acquired on white marble (grey line). (c) FORS spectra of two yellow areas (solid and dotted orange lines) compared to a reference spectrum of yellow ochre (black line). (d) XRF spectra of two brown areas (solid and dotted brown lines) compared to a spectrum acquired on white marble (grey line).

In the yellow areas, the FORS spectra (Figure 6c) showed the presence of iron hydroxides ($\text{Fe}_2\text{O}_3 \cdot \text{OH}, x\text{H}_2\text{O}$), confirmed by XRF spectra (not reported) in which the only signal (apart from that of calcium (Ca)) was that of iron (Fe). The FT-IR ATR analysis of a micro-sample (Table 2) taken from the yellow robe of Maria provided the definitive identification of the yellow pigment thanks to the characteristic bands at 905 and 795 cm^{-1} of goethite mineral ($\text{FeO}(\text{OH})$) [47,48]. Yellow ochre was used on the lid to paint the hair, and for both the bracelets and anklets of the cupids. In other Roman sarcophagi analyzed by the authors [23,24], yellow ochre was found as a priming layer for the gold leaf of the cupids' bracelets. Other scholars also describe the use of iron oxides and hydroxides either mixed or not with other materials, as a preparation layer for gilding [49,50]. In the case of the Lot Sarcophagus, no traces of gold were found. In the second register, yellow ochre was used for the hair and the cloth of the bride (left character in the shell), the cloth of Maria, and for several decorations such as a line on the wooden stick of Peter, the plumage of the rooster, the handle of Abraham's sword, the yellow line at the base of the altar, and the stars painted on the stones on the wall behind the characters. Yellow ochre was also one of the two pigments found in the third register, but only in the central scene, and it was used for the left cupid's hair in the tub with grapes in the Dionysian scene.

Clothes were also characterized by dark brown brushstrokes outlining the folds and the details. The XRF spectra acquired in correspondence of the brown brushstrokes on the yellow robes of the sister of Lazzaro and of the bride show iron signals (probably also due to the yellow layer below) and manganese (Mn) signals (Figure 6d). This brown color was widely used to highlight details, such as the nails of the hands or the studs of the reins of the donkey. The FORS spectrum (not shown here) acquired in correspondence with the brown line delimiting the nail on the groom's hand, an area without any colored layer below, showed the presence of brown iron–manganese-based pigment, most likely umber.

A huge amount of blue color traces was still visible, and VIL confirms that the pigment used was Egyptian blue. The identification was further confirmed by spot analyses (Figure 7g,h).

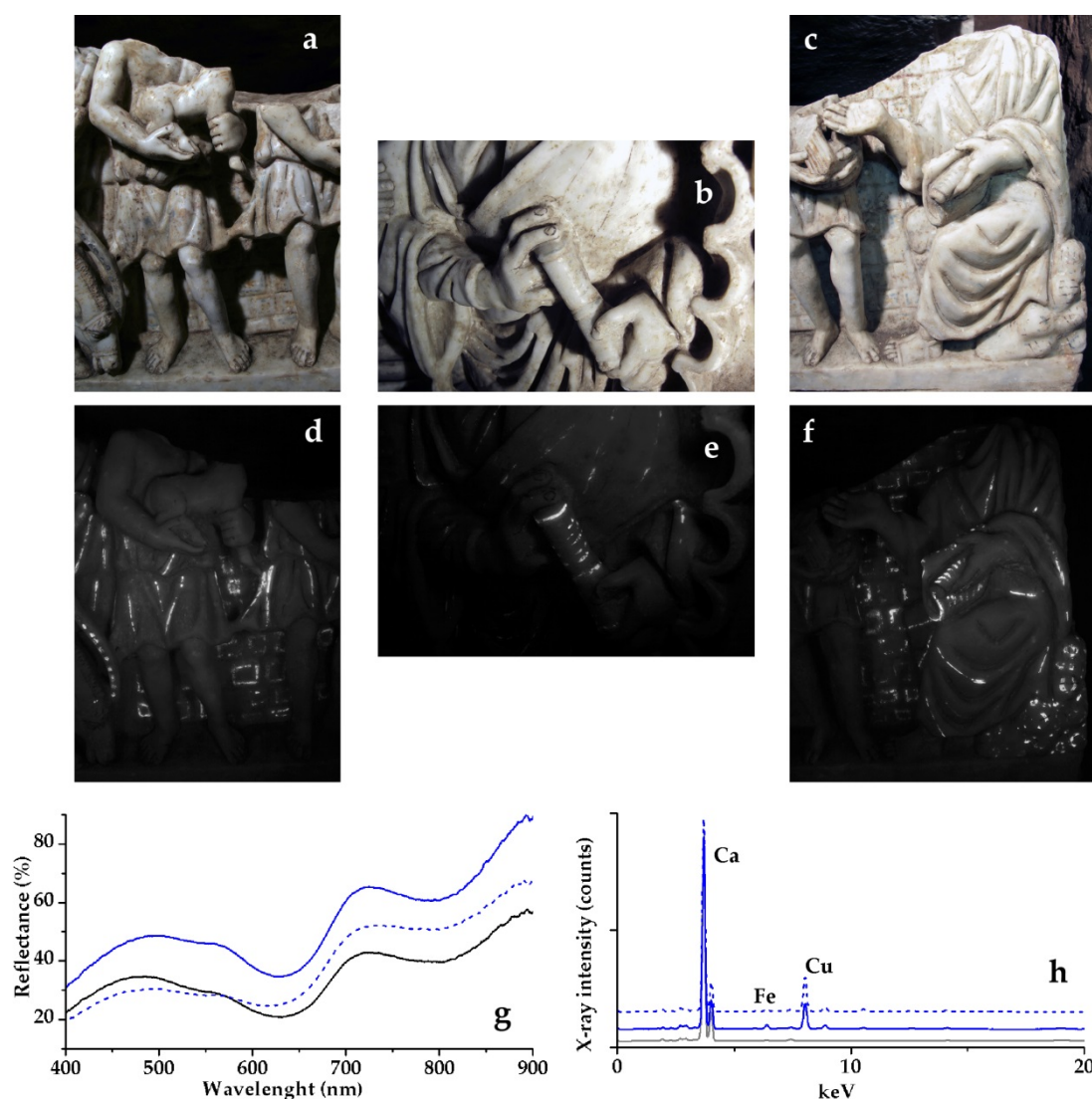


Figure 7. (a–c) Areas in visible light and (d–e) VIL images of the same areas. (g) FORS spectra of two blue areas (solid and dotted blue lines) compared to a reference spectrum of Egyptian blue (black line). (h) XRF spectra of two blue areas (solid and dotted blue lines) compared to a spectrum acquired on white marble (grey line).

The Egyptian blue was widely used on all surfaces of the sarcophagus starting from the lid, where it was used for the decoration of the edges, of the internal frame of the *tabula*, and for the wings of the cupids. In the second register, it was used for the clothes (Figure 7d), the decorations of the tomb of Lazarus, for the studs of the reins of the donkey (Figure 7d), and for the objects that the characters

hold in their hands, such as the groom's book (Figure 7e). It was also used to decorate the rock on which God the father sits and the wall behind the characters (Figure 7f).

In addition, in some areas where Egyptian blue was no longer visible to the naked eye, VIL was able to reveal its presence. As an example, Egyptian blue was found in the third register, in the Dionysian scene, in the eyes of the cupid on the left, outside the tube, and in an eye of the cupid in the center of the tube. Another important finding was the discovery of a wave-shaped decoration, with trefoil leaves, (Figure 8c,d) along the entire edge of the lid. It was interesting to note that the decoration continued also on the broken part (Figure 8d), thus proving that the pictorial decoration was done after the break took place.



Figure 8. (a,c) Areas in visible light and (c,d) VIL images of the edge of the lid showing the wave-shaped decoration painted with Egyptian blue.

Egyptian blue was also found, in a very small amount, in some purple decorations such as the left border of the sleeve and the small circles on the vest of Isaac, and some shadings on the plumage of the rooster. The XRF spectra (not reported here) showed signals of iron (Fe), mercury (Hg), and manganese (Mn), but not those of copper (Cu), most likely due to the low quantity of Egyptian blue present. Therefore, it was decided to take a microsample from the purple left border of the vest of Isaac to clarify the composition of this color (Table 2). SEM-EDS analyses of the cross section of the purple micro sample confirmed the data obtained with portable XRF and, in addition, the rare blue crystals in the layer showed signals of copper (Cu) and silica (Si). This purple color was thus obtained with a complex blend of umber, cinnabar, and Egyptian blue.

Furthermore, in the purple micro sample, there was no presence of any preparatory layer as well as in the sample of yellow color taken from the second register in correspondence with the robe of Maria (Table 2). This latter micro sample was already quoted before when yellow pigments were described.

In some areas of the lid and on the edge of the sarcophagus, a bright yellow UV luminescence was observable (Figure 2b). In Figure 9a,b, images of a detail of the edge of the sarcophagus in visible light and UVL are reported, respectively.

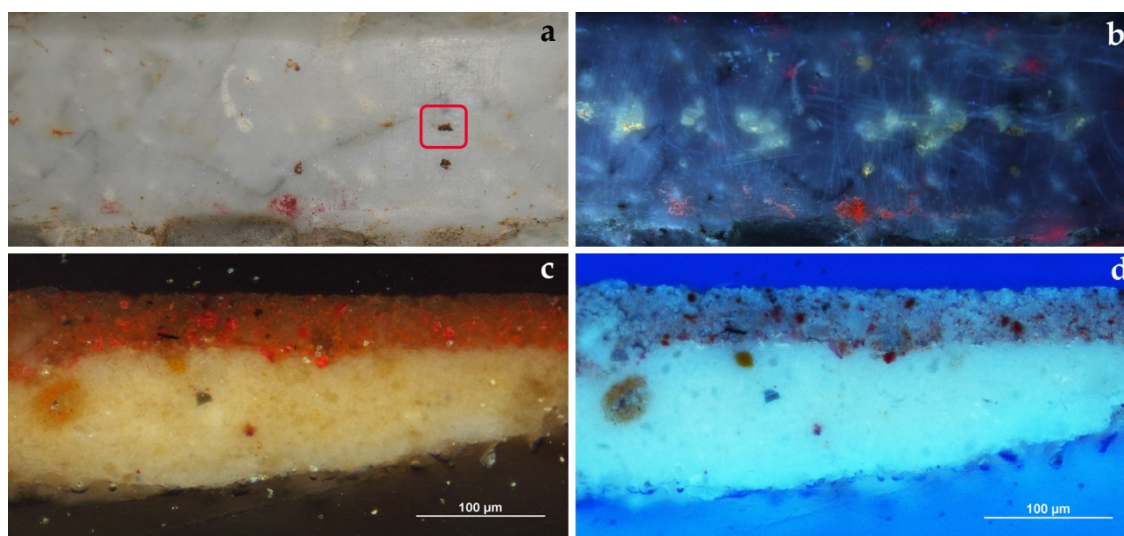


Figure 9. (a) Area in visible light and (b) in UVL of the upper edge of the sarcophagus. The red square in (a) indicates the sampling point. (c) Vis image and (d) UVL image of the cross section obtained from the microsample (magnification 20x, bar = 100 μm).

The XRF spectra, acquired on those areas, showed much more intense lead (Pb) signals than in the measured painted areas belonging to the second register. It has been reported that lead white pigments have photoluminescence properties [51], and therefore, it could be inferred that the UVL was due to the presence of lead white. Therefore, a microsample was taken from the upper edge of the sarcophagus to clarify these findings (Table 2). (Figure 9a, red square).

Unlike the other microsamples taken, in this latter a white, relatively homogeneous preparatory layer was present (Figure 9c). The EDS analyses showed almost only signals of lead (Pb), while iron (Fe) was present in the analyses of some, sporadic colored grains. The FT-IR spectrum of the preparatory layer highlighted the presence of the lead white, basic lead carbonate ($\text{Pb}(\text{CO}_3)\text{Pb}(\text{OH})_2$), by its characteristic absorption bands of 1407 and 684 cm^{-1} . The red layer was made of an admixture of cinnabar, red ochre, some lead white, and red lake. This latter, that in the VIS image is brilliant red (Figure 9c), in the UVL image appears pinkish (Figure 9d).

The use of the preparatory layer only on some parts, perhaps to impart to the decorative motifs a certain relief, is a rather rare finding and indicates precise choices by painters for obtaining specific results. Recently, the use of gypsum ($\text{CaSO}_4 \cdot 2\text{H}_2\text{O}$) as a priming layer has been reported for a 3rd century AC repainting on the *Ulpia Domnina* sarcophagus of the National Roman Museum in Rome, while the “original” painting (160–180 AC) was applied directly on the marble [50]. The high hiding power [52,53] of lead white renders the latter particularly suitable for tempera techniques on stone or marble. Notwithstanding this, the use of lead white for the preparatory layers was not so common in Roman sarcophagi. Lead white was found on painted Macedonian funerary monuments both as preparatory layers or blended with pigments to create different hues and enrich the palette of painters [54].

In the paper of 1951 [34], written shortly after the excavation of the sarcophagus, a rich polychromy was described, although the author underlines how this largely vanished in a short time². However,

² [...] Purtroppo, come suole avvenire, questa (la policromia) svani presto in gran parte al contatto con la luce e l'aria mossa e asciutta, volatilizzandosi dalla superficie estremamente pulita e lucida dei marmi, e restandone solo traccia nei solchi delle pieghe [...].

[...] Unfortunately, as usual, this (the polychromy) soon vanished largely on contact with the light and the moved and dry air, evaporating from the extremely clean and shiny surface of the marbles, and remaining only traces in the furrows of the folds [...].

in the detailed description of the polychromy, in addition to the colors and hues that were identified in this work, the presence of two green robes was mentioned (that of the groom and of Abraham). In this case, we were not successful, and no traces of any pigment (either green or blue and yellow) were found.

One of the very common problems emerging when studying the traces of polychromy is the identification of the binder which is, by its nature, the material that mostly undergoes degradation due to the passage of time and conditions in which the work was found. This being susceptible to degradation is also, in large part, the cause of the loss of polychromy.

In this case, the non-invasive techniques used *in situ* did not give any indication about the binder. Analyses of microsamples provided only a few hints. In the FT-IR spectra of the microsamples, no bands attributable to the binder (i.e., organic materials) were present. Again, this could be due to the low quantity present and thus below the sensitivity of the technique. In the SEM-EDS analyses of the three cross sections obtained from the three microsamples, beyond the elements correlated to the pigments, signals of phosphorus (P) were quite evident. Phosphorus is an element present in bone black [55]. Although no black crystals were present in the layers, the distribution of the phosphorus was uniform in the pictorial layers and not localized as it would be if due to bone black. These considerations lead to the hypothesis that phosphorus can be related to a binder such as casein, in which phosphoproteins are present [56].

For the 3D model, the three registers of the sarcophagus were reconstructed individually and subsequently aligned in a single model. About 40 photos were used for each register. By way of example, here, we describe the reconstruction of the second register. The 3D model reconstruction started with image alignment, in this first step, a sparse point cloud with 35,000 points was produced as an initial 3D representation of the scene. The second step increased the point cloud up to 6,000,000 points, and as the cloud directly derives from photographic images, it was colored.

Based on this last step, the software computes the reconstruction of the 3D polygonal mesh. After the geometry (mesh) is generated, it can be textured using the initial photos. Texture mapping is a way to add surface details, for example, color information, projecting one or more images onto the surface of the 3D model. As a result of the process, a model of 50,000,000 faces and a 3720 × 3720 pixel texture was created (Figure 10).



Figure 10. Two details of the digital model of the second register of the sarcophagus. (a) shell with bride and groom, (b) Isaac, servant with the donkey, Cain and Abel.

5. Conclusions

In this work, the surviving polychromy of the Lot Sarcophagus was studied *in-situ*, by applying mainly a non-invasive approach and using complementary portable techniques. Furthermore, some aspects not clarified by the non-invasive measures were clarified through a few targeted micro-samples.

The study allowed us to uniquely identify the rich palette used by the craftsmen who created this remarkable work of art, also revealing details that were no longer visible but important for the construction of the work. Moreover, the study, through the identification of extraneous incrustations and biological growth, provided useful information for both the choice of the cleaning method and for the future conservation. Indeed, the specific environmental conditions favored the development of cyanobacteria, and after the restoration, recolonization could be avoided by impeding the photosynthesis process by controlling the illumination quality, the cold light sources such as blue monochromatic lamp ($\lambda \sim 450$ nm) being recommended.

During the study of the sarcophagus, it was also understood that the use of polychromy completes the sculpture work. Some details are rendered only through color and not relief. In addition, the different decoration of the clothes helps to identify the main characters of the scenes. Therefore, the polychromy of the sculpture was not a subsequent addition but was integrated into the project of the work.

The Lot Sarcophagus is one of a kind, it is well known by scholars (archeologists and art historians) but very little by the general public because its location is not inserted in the museum path of the catacomb. With the disclosure of the data obtained from this study, using the acquired 3D model, the lack of knowledge can be overcome through special tools which are currently in preparation that will be available in the museum.

Color was, for the Romans, a question of civil status and the use of precious pigments had the meaning of emphasizing the social level of the costumer. In the case of wall paintings or polychrome statues in the *Domus*, the richness of the colors had to convey the message of luxury and high social status.

However, the colors, instead of being shown, were also hidden. This is the case of many objects, sarcophagi, and funeral slabs, present in the catacombs of Rome and thus visible to a few people. In the case of the Lot Sarcophagus, covered by layers of both mortar and masonry, the presence of the rich decoration was only for the deceased.

Author Contributions: Conceptualization, B.M. and S.B.; data acquisition, S.B., D.M., and R.M.d.F.; analysis and interpretation of data: S.B., D.M.; analysis and interpretation of biological data: O.A.C.; writing—original draft preparation, S.B.; writing—review and editing, S.B., D.M., R.M.d.F., O.A.C., and B.M.; funding acquisition, B.M. All authors have read and agreed to the published version of the manuscript.

Funding: This research was funded by The Heydar Aliyev Foundation, Azerbaijan.

Conflicts of Interest: The authors declare no conflict of interest.

References

1. Østergaard, J.S. Polychromy, sculptural, Greek and Roman. In *Oxford Classical Dictionary*; Oxford University Press: New York, NY, USA, 2020. Available online: oxfordre.com/classics (accessed on 12 June 2020).
2. *Polychromy in Ancient Sculpture and Architecture*; Bracci, S., Giachi, G., Liverani, P., Pallecchi, P., Paolucci, F., Eds.; Sillabe SrL: Livorno, Italy, 2018.
3. *I Colori del Bianco. Mille Anni di Colore Nella Scultura Antica*; Liverani, P. (Ed.) Coll. Studi e Docum.; De Luca Editori d'Arte, Roma, Musei Vaticani: Rome, Italy, 2015.
4. Hain, M.; Bartl, J.; Jacko, V. Multispectral analysis of cultural heritage artefacts. *Meas. Sci. Rev.* **2003**, *3*, 9–12.
5. Fischer, C.; Kakoulli, I. Multispectral and hyperspectral imaging technologies in conservation: Current research and potential applications. *Rev. Conserv.* **2006**, *7*, 3–16. [[CrossRef](#)]
6. Baldia, C.M.; Jakes, K.A. Photographic methods to detect colorants in archaeological textiles. *J. Archaeol. Sci.* **2007**, *34*, 519–525. [[CrossRef](#)]
7. Kakoulli, I.; Radpour, R.; Svoboda, M.; Fischer, C. Application of forensic photography for the detection and mapping of Egyptian blue and madder lake in Hellenistic polychrome terracottas based on their photophysical properties. *Dyes Pigment.* **2017**, *136*, 104–115. [[CrossRef](#)]

8. Bracci, S.; Magrini, D.; Iannaccone, R. The application of multi-band imaging integrated with non-invasive spot analyses for the examination of archaeological stone artefacts. In *Conservation 360°, UV-Vis Luminescence Imaging Techniques*; Picollo, M., Stols-Witlox, M., Fuster-López, L., Eds.; Editorial Universitat Politècnica de València: València, Spain, 2019; Volume 1, pp. 141–160. [CrossRef]
9. Bracci, S.; Vettori, S.; Cantisani, E.; Degano, I.; Galli, M. The ancient use of colouring on the marble statues of Hierapolis of Phrygia (Turkey): An integrated multi-analytical approach. *Anthropol. Archeol. Sci.* **2019**, *11*, 1611–1619. [CrossRef]
10. Rorimer, J.J. *Ultraviolet Rays and their Use in the Examination of Works of Art*; Metropolitan Museum of Art: New York, NY, USA, 1931.
11. Mairinger, F. The ultraviolet and fluorescence study of paintings and manuscripts. In *Radiation in Art and Archeometry*; Creagh, D.C., Bradley, D.A., Eds.; Elsevier: Amsterdam, The Netherlands, 2000; pp. 56–75. [CrossRef]
12. Pelagotti, A.; Pezzati, L.; Bevilacqua, N.; Vascotto, V.; Reillon, V.; Daffara, C.A. Study of UV fluorescence emission of painting materials. In Proceedings of the 8th International Conference on Non-Destructive Testing and Microanalysis for the Diagnostics and Conservation of the Cultural and Environmental Heritage, Lecce, Italy, 15–19 May 2005.
13. Pelagotti, A.; Pezzati, L.; Piva, A.; Del Mastio, A. Multispectral UV fluorescence analysis of painted surfaces. In Proceedings of the 14th European Signal Processing Conference (EUSIPCO), Florence, Italy, 4–8 September 2006.
14. Warda, J.; Frey, F.; Heller, D.; Kusheld, D.; Vitale, T.; Weaver, G. Ultraviolet photography. In *AIC Guide to Digital Photography and Conservation Documentation*, 2nd ed.; Warda, J., Ed.; American Institute for Conservation of Historic and Artistic Works: Washington, DC, USA, 2011.
15. Dyer, J.; Verri, G.; Cupitt, J. Multispectral Imaging in Reflectance and Photo-Induced Luminescence Modes: A User Manual. 2013. Available online: <http://www.britishmuseum.org/pdf/charisma-multispectral-imaging-manual-2013.pdf> (accessed on 3 March 2020).
16. Webb, E.K. UV-Induced Visible Luminescence for Conservation Documentation. In *Conservation 360°, UV-Vis Luminescence Imaging Techniques*; Picollo, M., Stols-Witlox, M., Fuster-López, L., Eds.; Editorial Universitat Politècnica de València: València, Spain, 2019; Volume 1, pp. 35–60. [CrossRef]
17. Riederer, J. Egyptian blue. In *Artist's Pigments. A Handbook of Their History and Characteristics*; Fitzhugh, E.W., Ed.; National Gallery of Art, Oxford University Press: New York, NY, USA, 1997; Volume 3, pp. 23–45.
18. Hatton, G.D.; Shortland, A.J.; Tite, M.S. The production technology of Egyptian blue and green frits from second millennium BC Egypt and Mesopotamia. *J. Archaeol. Sci.* **2008**, *35*, 1591–1604. [CrossRef]
19. Verri, G. The spatial characterisation of Egyptian blue, Han blue and Han purple by photo-induced luminescence digital imaging. *Anal. Bioanal. Chem.* **2009**, *394*, 1011–1021. [CrossRef]
20. Verri, G.; Saunders, D.; Ambers, J.; Sweek, T. Digital mapping of Egyptian blue: Conservation implications. *Stud. Conserv.* **2010**, *55*, 220–224. [CrossRef]
21. Verri, G. Broad-Band, Photo-Induced, Steady-State Luminescence Imaging in Practice. In *Conservation 360°, UV-Vis Luminescence Imaging Techniques*; Picollo, M., Stols-Witlox, M., Fuster-López, L., Eds.; Editorial Universitat Politècnica de València: València, Spain, 2019; Volume 1. [CrossRef]
22. Dyer, J.; Sotiropoulou, S. A technical step forward in the integration of visible-induced luminescence imaging methods for the study of ancient polychromy. *Herit. Sci.* **2017**, *5*, 24. [CrossRef]
23. Iannaccone, R.; Bracci, S.; Cantisani, E.; Mazzei, B. An integrated multi methodological approach for characterizing the materials and pigments on a sarcophagus in St. Mark, Marcellian and Damasus catacombs. *Appl. Phys. A* **2015**, *121*, 1235–1242. [CrossRef]
24. Liverani, P.; Bracci, S.; Iannaccone, R.; Lenzi, S.; Magrini, D.; Mazzei, B. Colours in the dark: New researches into catacombs. In *Polychromy in Ancient Sculpture and Architecture*; Bracci, S., Giachi, G., Liverani, P., Pallecchi, P., Paolucci, F., Eds.; Sillabe SrL: Livorno, Italy, 2018; pp. 111–121.
25. Miliiani, C.; Rosi, F.; Daveri, A.; Brunetti, B.G. Reflection infrared spectroscopy for the non-invasive in situ study of artists' pigments. *Appl. Phys. A* **2012**, *106*, 295–307. [CrossRef]
26. Bacci, M. Fiber optics applications to works of art. *Sens. Actuators* **1995**, *29*, 190–196. [CrossRef]
27. Bacci, M. UV-VIS-NIR, FT-IR, FORS Spectroscopies. In *Modern Analytical Methods in Art and Archaeology, Chemical Analysis Series*; Ciliberto, E., Spoto, G., Eds.; John Wiley and Sons: New York, NY, USA, 2000; Volume 155, pp. 321–362.

28. Aceto, M.; Agostino, A.; Fenoglio, G.; Idone, A.; Gulmini, M.; Picollo, M.; Ricciardi, P.; Delaney, J. Characterisation of colourants on illuminated manuscripts by portable fibre optic UV-Visible-NIR reflectance spectrophotometry. *Anal. Methods* **2014**, *6*, 1488–1500. [CrossRef]
29. Picollo, M.; Aceto, M.; Vitorino, T. UV-Vis spectroscopy. In *Chemical Analysis in Cultural Heritage*; Sabbatini, L., van der Werf, I.D., Eds.; De Gruyter: Berlin, Germany, 2020; pp. 253–271. [CrossRef]
30. Shugar, A.N.; Mass, J.L. *Handheld XRF for Art and Archaeology*; Leuven University Press: Leuven, Belgium, 2013.
31. Bezur, A.; Lee, L.; Loubser, M.; Trentelman, K. *Handheld XRF in Cultural Heritage*; J. Paul Getty Trust and Yale University: Los Angeles, CA, USA, 2020.
32. Karidas, A.G.; Brécoulaki, H.; Bourgeois, B.; Jockey, P. In Situ XRF Analysis of Raw Pigments and Traces of Polychromy on Marble Sculpture Surfaces. Possibilities and limitations. Available online: <https://bit.ly/3f4HYaq> (accessed on 27 July 2020).
33. Deichmann, F.W.; Bovini, G.; Brandenburg, H. *Repertorium der Christlich-Antiken Sarkophage. Erster Band. Rom und Ostia*; Franz Steiner Verlag: Wiesbaden, Germany, 1967; n. 188, Taf. 45.
34. Ferrua, A. Tre sarcofagi importanti da S. Sebastiano. *Riv. Archeol. Crist.* **1951**, *27*, 21–33.
35. Mazzei, B.; Di Gaetano, S. Il sarcofago di Lot in S. Sebastiano a Roma. Nuove osservazioni e spunti di riflessione scaturiti dal recente restauro. *Riv. Archeol. Crist.* **2019**, *95*, 35–74.
36. Westoby, M.J.; Brasington, J.; Glasser, N.F.; Hambrey, M.J.; Reynolds, J.M. 'Structure-from-Motion' photogrammetry: A low-cost, effective tool for geoscience applications. *Geomorphology* **2012**, *179*, 300–314. [CrossRef]
37. Rippka, R.; Deruelles, J.; Waterbury, J.B.; Herdman, M.; Stanier, R. Generic assignments, strain histories and properties of pure cultures of cyanobacteria. *J. Gen. Microbiol.* **1979**, *111*, 1–61. [CrossRef]
38. Komarek, J.; Anagnostidis, K. Cyanoprokaryota 1. Teil Chroococcales. In *Süßwasser-Flora von Mitteleuropa*; Ettl, H., Gärtner, G., Heynig, H., Mollenhauer, D., Eds.; Fisher Press: Stuttgart-Jena, Germany, 1998; Volume 19, pp. 1–548.
39. Komarek, J.; Anagnostidis, K. Cyanoprokaryota 2. Teil Oscillatoriales. In *Süßwasser-Flora von Mitteleuropa*; Büdel, B., Gärtner, G., Krienitz, L., Schagerl, M., Eds.; Elsevier GmbH Press: München, Germany, 2005; Volume 19, pp. 1–759.
40. Hernández Mariné, M.; Clavero, E.; Roldán, M. Why there is such luxurious growth in the hypogean environments. *Algol. Stud.* **2003**, *109*, 229–239. [CrossRef]
41. Montechiaro, F.; Giordano, M. Effect of prolonged dark incubation on pigments and photosynthesis of the cave-dwelling cyanobacterium *Phormidium autumnale* (Oscillatoriales, Cyanobacteria). *Phycologia* **2006**, *45*, 704–771. [CrossRef]
42. Bruno, L.; Belleza, S.; Urzi, C.; De Leo, F. A study for monitoring and conservation in the Roman Catacombs of St. Callistus and Domitilla, Rome (Italy). In *The Conservation of Subterranean Cultural Heritage*; Saiz-Jimenez, C., Ed.; Taylor & Francis Group: London, UK, 2014; pp. 37–44.
43. Luimstra, V.M.; Schuurmans, J.M.; Verschoor, A.M.; Hellingwerf, K.J.; Huisman, J.; Matthijs, H.C. Blue light reduces photosynthetic efficiency of cyanobacteria through an imbalance between photosystems I and II. *Photosynth. Res.* **2018**, *138*, 177–189. [CrossRef]
44. Clementi, C.; Doherty, B.; Gentili, P.L.; Miliani, C.; Romani, A.; Brunetti, B.G.; Sgamellotti, A. Vibrational and electronic properties of painting lakes. *Appl. Phys. A* **2008**, *92*, 25–33. [CrossRef]
45. Bisulca, C.; Picollo, M.; Bacci, M.; Kunzelman, D. UV-Vis-NIR reflectance spectroscopy of red lakes in paintings. In Proceedings of the 9th International Conference on NDT of Art Jerusalem, Jerusalem, Israel, 25–30 May 2008.
46. Elias, M.; Chartier, C.; Prévot, G.; Garay, H.; Vignaud, C. The colour of ochres explained by their composition. *Mater. Sci. Eng. B* **2006**, *127*, 70–80. [CrossRef]
47. Weckler, B.; Lutz, H.D. Lattice vibration spectra. Part XCV. Infrared spectroscopic studies on the iron oxide hydroxides goethite (α), akagankite (β), lepidocrocite (γ), and feroxyhite (δ). *Eur. J. Solid State Inorg. Chem.* **1998**, *35*, 531–544. [CrossRef]
48. Liu, H.; Chen, T.; Qing, C.; Xie, Q.; Frost, R.L. Confirmation of the assignment of vibrations of goethite: An ATR and IES study of goethite structure. *Spectrochim. Acta Part A* **2013**, *116*, 154–159. [CrossRef] [PubMed]

49. Sargent, M.L.; Therkildsen, R.H. The technical investigation of sculptural polychromy at the Ny Carlsberg Glyptotek 2009–2010—An Outline. In *Tracking Colour. The polychromy of Greek and Roman Sculpture in the NY Carlsberg Glyptotek. Preliminary Report 2*; Østergaard, J.S., Ed.; NY Carlsberg Glyptotek: Copenhagen, Denmark, 2010; pp. 11–26. Available online: <http://www.trackingcolour.com/publications/preliminary-reports> (accessed on 12 June 2020).
50. Siotto, E.; Dellepiane, M.; Callieri, M.; Scopigno, R.; Gratzu, C.; Moscato, A.; Burgio, L.; Legnaioli, S.; Lorenzetti, G.; Palleschi, V. A multidisciplinary approach for the study and the virtual reconstruction of the ancient polychromy of Roman sarcophagi. *J. Cult. Herit.* **2015**, *16*, 307–314. [[CrossRef](#)]
51. Gonzalez, V.; Gourier, D.; Calligaro, T.; Toussaint, K.; Wallez, G.; Menu, M. Revealing the origin and history of Lead-White pigments by their photoluminescence properties. *Anal. Chem.* **2017**, *89*, 2909–2918. [[CrossRef](#)]
52. Dunn, E.J., Jr. White hiding lead pigments. In *Pigments Handbook 1*; Patton, T.C., Ed.; John Wiley: New York, NY, USA, 1973; pp. 65–84.
53. Gettens, R.J.; Kuhn, H.; Chase, W.T. Lead White. In *Artists' Pigments. A Handbook of Their History and Characteristics*; Ashok, R., Ed.; Archetype Publication: London, UK, 1993; Volume 2, p. 70.
54. Brécoulaki, H. Sur la technè de la peinture grecque ancienne d'après les monuments funéraires de Macédoine. *Bull. Corresp. Hellénique* **2000**, *124*, 189–216. [[CrossRef](#)]
55. Winter, J.; FitzHugh, E.W. Pigments based on carbon. In *Artists' Pigments. A Handbook of Their History and Characteristics*; Berrie, B.H., Ed.; Archetype Publication: London, UK, 2007; Volume 4, p. 26.
56. Santamaria, U.; Morresi, F. Le indagini scientifiche per lo studio della cromia dell'Augusto di Prima Porta. In *I Colori del Bianco. Policromia Nella Scultura Antica, Collana di Studi e Documentazione*; Liverani, P., Ed.; Musei Vaticani De Luca Editori d'Arte: Rome, Italy, 2004; pp. 243–248.



© 2020 by the authors. Licensee MDPI, Basel, Switzerland. This article is an open access article distributed under the terms and conditions of the Creative Commons Attribution (CC BY) license (<http://creativecommons.org/licenses/by/4.0/>).